DMD Fast Forward. Published on March 3, 2021 as DOI: 10.1124/dmd.120.000264
This article has not been copyedited and formatted. The final version may differ from this version.

Title page:

SLCO1B1: Application and Limitations of Deep Mutational Scanning for Genomic Missense Variant Function.

Authors:

Lingxin Zhang, Vivekananda Sarangi, Ming-Fen Ho, Irene Moon, Krishna R. Kalari, *Liewei Wang, and *Richard M. Weinshilboum.

Division of Clinical Pharmacology, Department of Molecular Pharmacology and Experimental Therapeutics, Mayo Clinic, Rochester, MN. (L.Z., M.H., I.M., L.W., R.M.W.). Division of Biomedical Statistics and Informatics, Department of Health Sciences Research, Mayo Clinic, Rochester, MN. (V.S., K.R.K.). Mayo Clinic Center for Individualized Medicine, Mayo Clinic, Rochester, MN. (L.W., R.M.W.).

DMD Fast Forward. Published on March 3, 2021 as DOI: 10.1124/dmd.120.000264
This article has not been copyedited and formatted. The final version may differ from this version.

Running title page

a) Running title: High-throughput Characterization of *SLCO1B1* Variants of Unknown Significance.

b) Corresponding authors: *Drs. Weinshilboum and Wang are co-corresponding authors. Richard Weinshilboum, M.D., Mayo Clinic 200 First Street SW, Rochester, MN 55905, Phone: 507-284-2246 Email: weinshilboum.richard@mayo.edu; and Liewei Wang, M.D., Ph.D., Mayo Clinic 200 First Street SW, Rochester, MN 55905, Phone: 507-284-5264 Email: Wang.Liewei@mayo.edu.

c) Word count:

Number of text pages: 29

Number of tables: 1

Number of figures: 4

Number of words in abstract: 248

Number of words in introduction: 702

Number of words in discussion: 867

DMD Fast Forward. Published on March 3, 2021 as DOI: 10.1124/dmd.120.000264
This article has not been copyedited and formatted. The final version may differ from this version.

d) Abbreviations:

BFP, Blue fluorescent protein;

BWA, Burrows-Wheeler Aligner;

CPM, Counts per minute;

DMEM, Dulbecco's modified Eagle's medium;

DMS, Deep mutational scanning;

FACS, Fluorescence-activated cell sorting;

FBS, Fetal bovine serum;

GFP, Green fluorescent protein;

MAF, Minor allele frequency;

OATP1B1, Organic anion transporter protein 1B1;

ORF, Open reading frame;

NGS, Next generation sequencing;

SNP, Single nucleotide polymorphism;

SNV, Single nucleotide variant;

TM, Transmembrane;

WT, Wild-type.

DMD Fast Forward. Published on March 3, 2021 as DOI: 10.1124/dmd.120.000264
This article has not been copyedited and formatted. The final version may differ from this version.

Abstract

SLCO1B1 is an important transmembrane hepatic uptake transporter. Genetic variants in the *SLCO1B1* gene have been associated with altered protein folding, resulting in protein degradation and decreased transporter activity. Next-Generation Sequencing (NGS) of pharmacogenes is being applied increasingly to associate variation in drug response with genetic sequence variants. However, it is difficult to link variants of unknown significance with functional phenotypes using "one-at-a-time" functional systems. Deep mutational scanning (DMS) using a "landing pad cell-based system" is a high-throughput technique designed to analyze hundreds of gene open reading frame (ORF) missense variants in a parallel and scalable fashion. We have applied DMS to analyze 137 missense variants in the *SLCO1B1* ORF obtained from the ExAC Project. ORFs containing these variants were fused to green fluorescent protein and were integrated into "landing pad" cells. Florescence-activated cell sorting was performed to separate the cells into four groups based on fluorescence readout indicating protein expression at the single cell level. NGS was then performed and *SLCO1B1* variant frequencies were used to determine protein abundance. We found that six variants not previously characterized functionally displayed less than 25% and another twelve displayed approximately 50% of wild-type protein expression. These results were then functionally validated by transporter studies. Severely damaging variants identified by DMS may have clinical relevance for *SLCO1B1*-dependent drug transport but we need to exercise caution since the relatively small number of severely damaging variants identified raise questions with regard to the application of DMS to intrinsic membrane proteins such as *OATP1B1*.

DMD Fast Forward. Published on March 3, 2021 as DOI: 10.1124/dmd.120.000264
This article has not been copyedited and formatted. The final version may differ from this version.

Significance statement

The functional implications of a large numbers of ORF "variants of unknown significance" (VUS) in transporter genes have not been characterized. This study applied deep mutational scanning to determine the functional effects of VUS that have been observed in the ORF of *SLCO1B1*. Several severely damaging variants were identified, studied and validated. These observations have implications for both the application of DMS to intrinsic membrane proteins and for the clinical effect of drugs and endogenous compounds transported by *SLCO1B1*.

DMD Fast Forward. Published on March 3, 2021 as DOI: 10.1124/dmd.120.000264
This article has not been copyedited and formatted. The final version may differ from this version.

Introduction

The *SLCO1B1* gene encodes a trans-membrane organic anion transporter protein 1B1 (*OATP1B1*) that transports endogenous compounds such as 17-β-glucuronosyl estradiol and bilirubin as well as drugs such as statins and certain oral antidiabetic agents (Kitamura et al., 2008; van de Steeg et al., 2013). Genetic polymorphisms in or near a transporter gene can result in large individual variation in transporter facilitated drug uptake (Niemi, 2010; Oshiro et al., 2010). For example, the *SLCO1B1*5* missense variant (rs4149056) is associated with decreased plasma clearance of statins such as simvastatin, which can result in statin-induced myopathy (Giacomini et al., 2013). This same variant has been associated with increased plasma concentrations of estrone conjugates (Dudenkov et al., 2017; Moyer et al., 2018). The mechanism for decreased function associated with *SLCO1B1*5* may be related to alternation in its translocation to the cell membrane, as reported by previous studies (Kameyama et al., 2005; Voora et al., 2009). The Mayo Clinic recently completed the RIGHT 10K Pharmacogenomic study during which next generation sequencing (NGS) was performed using DNA from more than 10,000 Mayo Biobank participants to identify variants in 77 pharmacogenes, including *SLCO1B1* to make it possible to study the clinical implications of pharmacogenomic variants in these genes (Bielinski et al., 2014; Bielinski et al., 2020). The Exome Aggregation Consortium based at the Broad Institute has aggregated exome sequencing data for 60,706 individuals of diverse ancestries (Lek et al., 2016). Most of the variants observed in these subjects were variants of unknown significance (VUS). Most VUS—unlike common pharmacogenomics variants—are less frequent or rare, so they will be observed only occasionally in clinical practice, but when they do occur, their consequences can be highly clinically relevant. Therefore, the application of high throughput assays to begin

DMD Fast Forward. Published on March 3, 2021 as DOI: 10.1124/dmd.120.000264
This article has not been copyedited and formatted. The final version may differ from this version.

the process of determining which variants might have functional implications represents a significant step forward in terms of practical clinical utility.

Deep mutational scanning (DMS) is a technique that provides a platform with which a large number of missense variants can be interrogated in parallel, making it much more efficient than conventional "one variant at a time" methods (Matreyek et al., 2017). We recently functionally characterized 230 *CYP2C9* and *CYP2C19* missense variants using a DMS landing pad system. During those studies we identified and functionally validated a series of severely damaging variants (Zhang et al., 2020). Fowler et.al, pioneers in this field, and Yang et.al have used this landing pad system to study the function of a series of important proteins such as *TMPT*, *PTEN* and *NUDT15*, all of which are primarily located in the cytosol (Matreyek et al., 2018; Suiter et al., 2020). Although the *OATP1B1* transporter is an intrinsic membrane protein, one of the mechanisms that regulates transporter activity involves variation in protein expression as a result of lysosome-mediated or other mechanisms for protein degradation (Alam et al., 2016). We should also note the limited applicability of DMS for the study of missense variants leading to loss-of function via other mechanisms such as variants that result in changes in subcellular localization or post-translational regulation.

In the present study, we set out to analyze the functional implications of missense variants that have been observed in the *SLCO1B1* open reading frame (ORF). We analyzed 137 missense variants that have been observed in the ORF of this gene (Lek et al., 2016). Specifically, we included genetic variants with minor allele frequencies (MAF) >0.00001 as reported by the Exome Aggregation Consortium as well as novel ORF VUS observed by the Mayo Right 10K Project.

DMD Fast Forward. Published on March 3, 2021 as DOI: 10.1124/dmd.120.000264
This article has not been copyedited and formatted. The final version may differ from this version.

We found that 6 of the 137 *SLCO1B1* missense variants that we studied displayed less than approximately 25% of wild-type (WT) protein expression, a level that might significantly decrease transporter activity. We also compared variant functional information determined by DMS with the predictions of computational algorithms and, finally, we experimentally validated variants found to be severely damaging by the use of Western blot analysis and transport studies. Our findings indicate that DMS can be an efficient high-throughput method for the identification of low protein abundance ORF VUS that might have potential clinical implications for drug transport. However, they also suggest that caution will have to be exercised in the interpretation of this type of data for intrinsic membrane proteins like *OATP1B1*.

DMD Fast Forward. Published on March 3, 2021 as DOI: 10.1124/dmd.120.000264
This article has not been copyedited and formatted. The final version may differ from this version.

Materials and methods

Generation of DMS variant library

The landing pad cell line clone#20 with a single landing pad was previously generated in order to integrate *SLCO1B1* expression cassettes, and *SLCO1B1* promotor-less cassettes were created by Gibson Assembly as previously described (Zhang et al, 2020). The attachment site (attB) on promoter-less cassettes and the plasmid attachment site (attP) on landing pad clone#20 were integrated by using Bxb1 recombinase. Human *SLCO1B1* ORF cDNA plasmids were obtained from Genscript (Piscataway, NJ). Nicking mutagenesis methods were modified from Wrenbeck et.al (Wrenbeck et al., 2016) to construct variant libraries for ORFs containing *SLCO1B1* missense variants. Phosphorylated oligonucleotides for *SLCO1B1* variants were purchased from IDT (Coralville, IW). Sanger sequencing was used to validate sequences of the variant clones.

Cell culture and plasmid transfection

HEK 293T cells were cultured in Dulbecco's modified Eagle's medium (DMEM) supplemented with 10% fetal bovine serum (FBS), 100 μg/ml penicillin, and 0.1 mg/ml streptomycin. Long-term passage of the landing pad cell line used the media described above with 2 μg/ml doxycycline (Sigma-Aldrich, St.Louis, MO). Doxycycline medium was removed one day before adding Bxb1 recombinase by transfection. The expression vector pCAG–NLS–HA–Bxb1 (Addgene #51271) was used to express Bxb1 recombinase mediated integration of variant libraries performed with plasmid DNA using 5×10^5 cells transfected with 3 μg of plasmid DNA using 6 μL of Fugene6 (Promega, Fitchburg, WI) in a six-well plate.

DMD Fast Forward. Published on March 3, 2021 as DOI: 10.1124/dmd.120.000264
This article has not been copyedited and formatted. The final version may differ from this version.

Fluorescence-activated cell sorting

The promoter less attB-*SLCO1B1* plasmids, as shown graphically in **Figure 1A**, were transfected 24 hours after recombinase Bxb1 transfection on landing pad clone#20. The expression of BFP (blue fluorescence protein) on landing pad cells was inducted by doxycycline. After 5 days, candidate clones were trypsinized, washed with PBS and were fixed in 4% formaldehyde at 4 °C for 10 min. The cells were analyzed by flow cytometer FACS CantoX (BD Biosciences, San Jose, CA) and by the use of FACSDiva v8.0 software and Flowjo software v10 (BD Biosciences, San Jose, CA). The FACS CantoX instrument utilizes colinear 405 nm, 488 nm and 561 nm lasers plus forward and side angle light scatter. Library cells were washed, trypsinized, and resuspended in PBS containing 5% FBS. Cells were then sorted into four bins using a FACSAria with 407 nm, 488 nm, and 532 nm lasers (BD Biosciences), and the cells were collected in culture medium. $BFP^-/mCherry^+$ cells containing *SLCO1B1* variants were flow sorted and grown for 5 days. $BFP^-/mCherry^+$ cells were sorted again to determine the protein expression of *SLCO1B1* variants based on their GFP/mCherry ratios. Gates were set based on GFP/mCherry ratios for cells integrating known *SLCO1B1* variants and WT proteins as gating references. Four gates were set to dissect the pooled libraries into four different bins based on GFP/mCherry ratios. The data were analyzed by FACS Diva v8.0.1 software.

Sequencing library preparation and sequencing

Amplicons for *SLCO1B1* were amplified from 250 ng genomic DNA using KAPA HiFi HotStart ReadyMix (Kapa Biosystems, Willmington, MA). Primers were designed to bind to common

DMD Fast Forward. Published on March 3, 2021 as DOI: 10.1124/dmd.120.000264
This article has not been copyedited and formatted. The final version may differ from this version.

non-mutated regions of the cassette sequences. PCR products were purified by use of the QIAquick PCR Purification Kit (Qiagen, Germany) and were quantified by Qubit® dsDNA HS Reagent (Fisher Scientific, Hampton, NH). The amplicon DNA (1 ng) was used as the starting material for library preparation by use of the Nextera XT DNA Preparation Kit (Illumina, San Diego, CA). Barcode adapters (Genewiz, South Plainfield, NJ) were used for library preparation; and samples were pooled after indexing and were sequenced using the Illumina HiSeq4000 Sequencing System in rapid run mode using the TruSeq Rapid SBS Kit (Illumina, San Diego, CA) with 300-cycle and 2 X 150bp paired-end read capability. Files were aligned to the *SLCO1B1* reference sequence.

Variant calling

The fastq files were aligned with the *SLCO1B1* reference sequence using Burrows-Wheeler Aligner (BWA) version 0.7.15. Samtools mpileup version 1.5 was used together with a custom python script for single nucleotide variant (SNV) calling. A base quality score cut-off of 20 and a mapping quality score cut-off of 20 were applied for SNV calling. Custom scripts were used to summarize the data and add allele frequencies for each base at all positions in the reference sequence, **Supplemental Script 1**.

Western blots

$BFP^-/mCherry^+$ cells containing individual *SLCO1B1* variants were lysed and proteins were separated by SDS-PAGE prior to transfer to PVDF membranes. The membranes were incubated

DMD Fast Forward. Published on March 3, 2021 as DOI: 10.1124/dmd.120.000264
This article has not been copyedited and formatted. The final version may differ from this version.

with rabbit polyclonal *OATP1B1* antibody directed against a recombinant fragment corresponding to human *OATP1B1* aa426-537. (Abcam, Cat. No.ab224610) at a 1:1000 dilution. mCherry protein was measured using mouse monoclonal mCherry antibody at a 1:2000 dilution (Sigma, Cat. No. SAB2702291), and its expression was used as a loading control. Proteins were detected using the SuperSignal™ West Dura Extended Duration Substrate (Thermo Scientific, Waltham, MA), and Western blot images were captured by use of the ChemiDoc™ Touch Image System (Bio-Rad, Hercules, CA).

Transporter assay

Radioactively labeled estradiol 17-β-D-glucuronide [Estradiol-6,7-^{3}H(N)] 51.5Ci/mmol (PerkinElmer, Boston, MA) was used to measure the uptake of this compound by *SLCO1B1* transporter variants. Specifically, BFP^{-}/$mCherry^{+}$ cells were seeded at a density of 4 x 10^{5} cells/well on 24-well plates and were grown to confluence for 24 hours (van de Steeg et al., 2013). Prior to the start of the experiment, cells were washed twice with prewarmed Hanks' balanced salt solution HBSS/HEPES (pH 7.4) buffer, and were incubated with increasing concentrations of [^{3}H]-labeled estradiol 17-β-D-glucuronide ranging from 1.5 nM to 48 nM for 1 min. The highest concentration that we used was higher than the physiological range but this concentration range was used for the *in vitro* uptake study (Parvez et al., 2016). Uptake was terminated by washing the cells with 0.4 ml ice-cold HBSS/HEPES plus 0.5% bovine serum albumin and twice with 0.4 ml ice-cold HBSS/HEPES, followed by the addition of 200 µL M-per buffer per well (Thermo Scientific, Waltham, MA). The cell lysate (150 uL) was transferred to a 5-ml plastic scintillation vial for the measurement of radioactivity by liquid scintillation

DMD Fast Forward. Published on March 3, 2021 as DOI: 10.1124/dmd.120.000264
This article has not been copyedited and formatted. The final version may differ from this version.

counting (Beckman Coulter, Indianapolis, IN). Protein concentrations for each sample were measured using the Bradford method (BioRad, Hercules, CA). The amount of radioactively labeled estradiol 17-β-D-glucuronide that accumulated within the cells was determined by using liquid scintillation counting. The data were expressed in counts per minute (CPM) normalized by the protein content in milligrams.

DMD Fast Forward. Published on March 3, 2021 as DOI: 10.1124/dmd.120.000264
This article has not been copyedited and formatted. The final version may differ from this version.

Results

Generation of *SLCO1B1* variant libraries

We utilized the high-throughput DMS system to study the protein expression of 137 *SLCO1B1* missense variants. The DMS system includes a landing pad cell line and promoter-less *SLCO1B1* cassettes. Landing pad cell line clone#20 with a single landing pad was used in these studies, as described in our previous publication (Zhang et al., 2020). Briefly, this landing pad cell line was generated using HEK293T cells which have been reported to have hypotriploid karyotypes. Therefore, we screened different clones and found clone#20 with one copy of the landing pad, which enabled us to integrate a single *SLCO1B1* variant per cell (Zhang et al., 2020). A promotor-less *SLCO1B1* cassette was constructed that included the *SLCO1B1* ORF sequence and C-terminal of the ORF was fused with GFP to indicate protein expression (**Figure 1A)**. mCherry was expressed after the IRES component, which was used as a control for transfection. Once the *SLCO1B1* ORF cassette landed on the landing pad by use of the Bxb1 recombinase, blue fluorescent protein (BFP) in landing pad cells was disrupted and the $BFP^-/mCherry^+$ cells were collected for flow cytometry or FACS analysis performed in the subsequent experiments. GFP/mCherry ratios were used as an indicator for *SLCO1B1* protein expression in the DMS system. In an earlier study (Tirona et al., 2001), using Western blotting alone had shown that the *SLCO1B1*2* (rs56101265) variant allele affected final transporter protein quantity. For *SLCO1B1*2* , the mean GFP/mCherry ratios was 61.5% of WT GFP/mCherry ratios, in a good agreement with the Western blot results in the Tirona et.al. publication (see **Figure 1B**). These results were used as flow cytometry gating controls for subsequent experiments. Specifically, we used nicking mutagenesis to create 137 *SLCO1B1* missense variants with a MAF higher than 0.001% from Exome Aggregation Consortium and the Mayo Clinic Right 10K Project. The

DMD Fast Forward. Published on March 3, 2021 as DOI: 10.1124/dmd.120.000264
This article has not been copyedited and formatted. The final version may differ from this version.

pooled *SLCO1B1* variants expression cassettes were integrated into landing pad cells clone#20. As the next step, we used the known damaging *SLCO1B1*2* variant together with the WT *SLCO1B1* construct as references to establish FACS gating. Specifically, the *SLCO1B1* variant libraries were FACS sorted into four different "bins" based on the values of GFP/mCherry ratios, which was an indicator of the protein expression for each variant, i.e. the higher that ratio, the more was the protein abundance of the expressed *SLCO1B1* variant (**Figure 1C**). We used three categories of variant classification, "severely damaging" variants in bin 1, "damaging" variants in bins 2 and 3 or "tolerated" variants in bin 4 on the basis of flow cytometry validation (**Figure 1C and D**). The DMS system, as shown in **Figure 1**, made it possible to determine the quantity of variant protein expressed for each of the variants encoded by constructs containing VUS.

Effect of *SLCO1B1* variants on protein levels

Pools of $BFP^-/mCherry^+$ cells expressing *SLCO1B1* missense variants were sorted by four-way FACS sorting as shown in **Figure 1D**. DNA was extracted from the cells collected in each bin and was then subjected to NGS amplicon sequencing. Variant frequencies for each variant in each bin were called by custom scripts (see **Supplemental Script 1)**. Abundance scores for each *SLCO1B1* individual variant were determined using the following equation in which Fv = variant frequency of the *SLCO1B1* variant in each bin:

$$\text{Abundance score} = \frac{(F_{v,bin1}\times 0.25)+(F_{v,bin2}\times 0.5)+(F_{v,bin3}\times 0.75)+(F_{v,bin4}\times 1)}{(F_{v,bin1}+F_{v,bin2}+F_{v,bin3}+F_{v,bin4})}$$

The "abundance score" for each variant was calculated by multiplying Fv with weighted values from 0.25 to 1 across the four bins, with the weighted values being assigned on the basis of the percentage of protein expression compared to WT (Fowler and Fields, 2014; Matreyek et al.,

DMD Fast Forward. Published on March 3, 2021 as DOI: 10.1124/dmd.120.000264
This article has not been copyedited and formatted. The final version may differ from this version.

2017; Matreyek et al., 2018; Zhang et al., 2020). The mean abundance score for each individual variant was calculated based on at least three independent replicate assays. The abundance scores for *SLCO1B1* variants shown graphically in **Figure 2** and in **Supplemental Figure S1** and **Table S1**. "Severely damaging" variants fell into bin 1, "damaging" variants fell into bin 2 and bin 3 and "tolerated" variants fell into bin 4 on the basis of the flow cytometry results. Specifically, "severely damaging" *SLCO1B1* variants had approximately 25% protein expression or less as compared to WT, with abundance scores of less than 0.5768 (*SLCO1B1*1B* 388A>G, rs2306283), while variants with abundance scores equal to or above that threshold but lower than 0.6015 (*SLCO1B1*27* 1200C>G, rs59113707) were considered as "damaging", expressing approximately 50% of the *OATP1B1* WT protein abundance. As a result, *SLCO1B1* variants with abundance scores above 0.6015 were categorized as "tolerated" (**Figure 2**). In summary, we performed FACS to separate the cells into four bins based on fluorescence readout. The amplicon sequencing of DNA in each bin, followed by computational analysis of variant frequencies in each bin was then used to determine the level of *OATP1B1* expression for constructs expression each VUS (**Figure 3)**. We observed six severely damaging *SLCO1B1* variants (1462G>A, 1246G>A, 215G>A, 1508A>G 1828C>T, and 1296C>A) as determined by abundance scores calculated from variant frequencies.

Using DMS, the variant calling results for 137 *SLCO1B1* variants (MAF > 0.00001) from the ExAC browser (current gnomAD database) and *SLCO1B1* variants from the Mayo RIGHT 10K Study are also listed in the order of classification of variants from DMS results in **Figure 5**. In addition, we compared the DMS results with other prediction algorithms using SIFT, Provean, Polyphen2 and CADD, and found two severely damaging variants (215G>A and 1296C>A) and

DMD Fast Forward. Published on March 3, 2021 as DOI: 10.1124/dmd.120.000264
This article has not been copyedited and formatted. The final version may differ from this version.

eight damaging variants (388A>G, 1200C>G, 671T>A, 1015G>C, 235 C>T, 38C>A, 991A>G, and 154A>G) that were identified by the DMS method that were missed by one of the four algorithms. Those results are listed in **Supplemental Table S3**. We also searched PharmVar, a database that includes, among other information, the possible impact of pharmacogenetic sequence variation on drug response, but that database does not include reports of the function of these variants (Gaedigk et al., 2018). One of the six severely damaging variants was shown in **Figure 3**, *SLCO1B1* c.1296C>A, rs534931824, which had a MAF of 0.01%, might also provide clinically useful information.

Functional Validation of *SLCO1B1* severely damaging variants

We next attempted to confirm our results for the severely damaging variants that we identified by DMS by the use of functional studies. We validated the protein expression data for these newly identified severely damaging variants (1462G>A, 1246G>A, 215G>A, 1508A>G, 1828C>T, and 1296C>A) by applying Western blot analyses, the results are shown in **Figure 4A**. The six variants for *SLCO1B1* predicted to be severely damaging displayed less than 25% protein expression when compared to the *OATP1B1* WT protein. *SLCO1B1*2* and *SLCO1B1*5* were also studied as comparators. Finally, we performed transporter assays to determine the transporter activity of these newly identified severely damaging variants. Transport by the severely damaging variants was significantly decreased when compared to the WT protein as measured by the uptake of radioactive 17-estradiol β-D-glucuronide, a prototypic substrate for transport by *SLCO1B1*. The concentration-dependent 17-estradiol β-D-glucuronide uptake by severely damaging variants and WT *OATP1B1* protein are shown graphically in **Figure 4B**. All six newly identified functional *SLCO1B1* variants revealed significantly lower transporter

DMD Fast Forward. Published on March 3, 2021 as DOI: 10.1124/dmd.120.000264
This article has not been copyedited and formatted. The final version may differ from this version.

activities, as shown in **Figure 4B** and by the bar graph in **Figure 4C**, which depicts the level of reduction in transport at optimal concentrations of radioactive 17-estradiol β-D-glucuronide. Protein degradation of variants represents a common mechanism by which missense variants can alter protein abundances and, as a result, transport function. However, there are also examples in which alterations in transport are clearly not related to variation in transporter protein quantity. For example, *SLCO1B1*5* displays WT-like protein abundance but is associated with decreased transporter activity. The mechanism for decreased function associated with *SLCO1B1*5* may be related to alternation in its translocation to the cell membrane as reported previously (Kameyama et al., 2005; Voora et al., 2009). The amino acid changed by the **5* variant maps to *SLCO1B1* transmembrane domain 4 (TM4), so we also studied transport of a prototypic *SLCO1B1* substrate by eight additional variants which we studied that mapped to the same transmembrane domain. We found that, of the eight variants with WT-like abundance scores, six displayed normal or even elevated transport but two (*SLCO1B1* 529G>C and 560C>T) displayed relatively decreased transporter capacity, as shown in **Figure 4D** and by the bar graph in **Figure 4E** which depict the transporter activities at 24 nM radioactive 17-estradiol β-D-glucuronide. These observations suggest that these additional two variants in TM4 may also display impaired transport just as does *SLCO1B1*5.* Furthermore, two variants (*SLCO1B1* 508A>T and 577C>T) show significantly increased activity as compared to WT, tested statistically by one-way ANOVA $p<0.05$, as shown in **Figures 4E**.

DMD Fast Forward. Published on March 3, 2021 as DOI: 10.1124/dmd.120.000264
This article has not been copyedited and formatted. The final version may differ from this version.

Discussion

There have been functional studies of a limited number of clinically relevant *SLCO1B1* drug transporter variants which have applied "one-at-a-time" systems that are labor-intensive and which require time-consuming assays. In this study, we have used the DMS landing pad platform to functionally characterize naturally occurring ORF missense variants for *SLCO1B1* in a high-throughput fashion (Fowler and Fields, 2014; Matreyek et al., 2017; Matreyek et al., 2018; Zhang et al., 2020). The landing pad cell line clone#20 with a single landing pad was used in order to screen variant protein expression in a high-throughput manner (Zhang et al., 2020). Missense variants in *SLCO1B1* may result in altered protein expression as a result of proteasome or lysosome-mediated degradation, a major mechanism responsible for decreased protein expression for pharmacogenomic variants (Wang et al., 2004; Alam et al., 2016; Matreyek et al., 2018; Suiter et al., 2020; Zhang et al., 2020). Loss of function by variants containing non-synonymous *SLCO1B1* ORF SNPs due to decreased protein expression made it possible for us to analyze that function by the use of fluorescence reporter assays. FACS sorting was used to separate variants associated with differing protein expression levels, all of which were subsequently identified by NGS to make it possible to calculate the frequency of each of the variants. We chose to study focused variant libraries, that is, libraries that included variants above a specified level of natural occurrence rather than using saturation mutant libraries for *SLCO1B1* missense variants. Specifically, we analyzed 137 non-synonymous ORF variants for *SLCO1B1* from the ExAC study that had MAF >0.00001 (see **Figure 2**) (Lek et al., 2016). We validated the transporter activities for severely damaging variants and those results were in good agreement with protein expression levels, as shown in **Figure 4A**. The crystal structure of *SLCO1B1* has not yet been reported, but twelve transmembrane domains (TM) have been

DMD Fast Forward. Published on March 3, 2021 as DOI: 10.1124/dmd.120.000264
This article has not been copyedited and formatted. The final version may differ from this version.

identified in *OATP1B1* transporter sequences (Hong et al., 2010). Five of our six newly identified severely damaging variants were located in intracellular loops or extracellular in non-membrane domains. In silico predictions with regard to how damaging individual variants might be were not always consistent with our DMS results, as shown in **Supplemental Table 3**, and previous publication suggested that decreased protein expression of *SLCO1B1* variants is only one of the mechanisms that can result in impaired function (Kameyama et al., 2005). Obviously, proteins that include *SLCO1B1* non-synonymous variants can display WT-like protein abundance joined with decreased transporter activity. That fact is emphasized in dramatic fashion by *SLCO1B1 *5* which displayed significantly reduced transporter activity, together with a protein level similar to that of WT *SLCO1B1*. The list of variants included in the study included eight variants that mapped to gene sequence encoding TM4, the domain that includes *SLCO1B1*5*. Most of those TM4 variants displayed WT-like or higher levels of transport, but two of the eight showed decreased transport (see **Figure 4C**). One possible limitation of the use of DMS to study *OATP1B1* and other intrinsic membrane proteins might be related to the fact that mechanisms for loss of function or decreased activity for these proteins may be missed by the type of assay which we applied—i.e. protein expression. *In silico* predictions have been widely applied to predict variation in protein function that has implications for pharmacogenomics and other aspects of drug effect (Flanagan et al., 2010; Kircher et al., 2014; Choi and Chan, 2015; Vaser et al., 2016). Our own previous work and that of others supports the importance of the application of a variety of functional methods to validate results obtained by using predictive algorithms. Therefore, we compared calling variant function by the use of DMS with the predictions of computational algorithms, and significant differences were found between our results and those of predictive algorithms, differences which may due to underlying

DMD Fast Forward. Published on March 3, 2021 as DOI: 10.1124/dmd.120.000264
This article has not been copyedited and formatted. The final version may differ from this version.

molecular mechanisms responsible for *SLOC1B1* decreased function, as listed in **Supplemental Table S3**.

Based on our results and the experience of other groups, DMS appears to be a useful and sensitive method for the study of cytosolic proteins such as *TMPT*, *PTEN* and *NUDT15* and of endoplasmic reticulum proteins such as *CYP2C9* and *CYP2C19*, for which a major mechanism of loss-of-function is protein degradation in which case damaging variants would be expected to display clear fluorescence separation from WT-like variants (Wang et al., 2005; Li et al., 2008; Matreyek et al., 2018; Devarajan et al., 2019; Suiter et al., 2020). The functional implications of genetic variation that alters amino acid sequence in the *SLCO1B1* gene is clearly a complex process involving multiple mechanisms, which could include changes in plasma membrane localization and integration, protein degradation as well as transcriptional and post-translational variation (Alam et al., 2016; Alam et al., 2018). For intrinsic transmembrane proteins like *OATP1B1*, DMS may be one of a series of methods that will be needed to predict alterations in *SLCO1B1* function.

In summary, we have identified and validated six *SLCO1B1* severely damaging variants that had not previously been reported in PharmVar. Those variants are potentially actionable clinically if they can be linked to individual variation in drug response phenotypes or disease pathophysiology. Functional studies of the variants that we found to display decreased protein expression supported the functional consequences predicted by DMS.

DMD Fast Forward. Published on March 3, 2021 as DOI: 10.1124/dmd.120.000264
This article has not been copyedited and formatted. The final version may differ from this version.

Author Contributions

Participated in research design: Zhang, Ho, Wang and Weinshilboum.

Conducted experiments: Zhang, Moon.

Performed data analysis: Zhang, Sarangi, R. Kalari.

Contributed to the writing of the manuscript: Zhang, Ho,and Weinshilboum.

DMD Fast Forward. Published on March 3, 2021 as DOI: 10.1124/dmd.120.000264
This article has not been copyedited and formatted. The final version may differ from this version.

References

Alam K, Crowe A, Wang X, Zhang P, Ding K, Li L, and Yue W (2018) Regulation of Organic Anion Transporting Polypeptides (OATP) 1B1- and OATP1B3-Mediated Transport: An Updated Review in the Context of OATP-Mediated Drug-Drug Interactions. *Int J Mol Sci* **19**.

Alam K, Pahwa S, Wang X, Zhang P, Ding K, Abuznait AH, Li L, and Yue W (2016) Downregulation of Organic Anion Transporting Polypeptide (OATP) 1B1 Transport Function by Lysosomotropic Drug Chloroquine: Implication in OATP-Mediated Drug-Drug Interactions. *Mol Pharm* **13:**839-851.

Bielinski SJ, Olson JE, Pathak J, Weinshilboum RM, Wang L, Lyke KJ, Ryu E, Targonski PV, Van Norstrand MD, Hathcock MA, Takahashi PY, McCormick JB, Johnson KJ, Maschke KJ, Rohrer Vitek CR, Ellingson MS, Wieben ED, Farrugia G, Morrisette JA, Kruckeberg KJ, Bruflat JK, Peterson LM, Blommel JH, Skierka JM, Ferber MJ, Black JL, Baudhuin LM, Klee EW, Ross JL, Veldhuizen TL, Schultz CG, Caraballo PJ, Freimuth RR, Chute CG, and Kullo IJ (2014) Preemptive genotyping for personalized medicine: design of the right drug, right dose, right time-using genomic data to individualize treatment protocol. *Mayo Clin Proc* **89:**25-33.

Bielinski SJ, St Sauver JL, Olson JE, Larson NB, Black JL, Scherer SE, Bernard ME, Boerwinkle E, Borah BJ, Caraballo PJ, Curry TB, Doddapaneni H, Formea CM, Freimuth RR, Gibbs RA, Giri J, Hathcock MA, Hu J, Jacobson DJ, Jones LA, Kalla S, Koep TH, Korchina V, Kovar CL, Lee S, Liu H, Matey ET, McGree ME, McAllister TM, Moyer AM, Muzny DM, Nicholson WT, Oyen LJ, Qin X, Raj R, Roger VL, Rohrer Vitek CR, Ross JL, Sharp RR, Takahashi PY, Venner E, Walker K, Wang L, Wang Q, Wright JA, Wu TJ, Wang L, and Weinshilboum RM (2020) Cohort Profile: The Right Drug, Right Dose, Right Time: Using Genomic Data to Individualize Treatment Protocol (RIGHT Protocol). *Int J Epidemiol* **49:**23-24k.

Choi Y and Chan AP (2015) PROVEAN web server: a tool to predict the functional effect of amino acid substitutions and indels. *Bioinformatics* **31:**2745-2747.

Devarajan S, Moon I, Ho MF, Larson NB, Neavin DR, Moyer AM, Black JL, Bielinski SJ, Scherer SE, Wang L, Weinshilboum RM, and Reid JM (2019) Pharmacogenomic Next-Generation DNA Sequencing: Lessons from the Identification and Functional Characterization of Variants of Unknown Significance in CYP2C9 and CYP2C19. *Drug Metab Dispos* **47:**425-435.

Dudenkov TM, Ingle JN, Buzdar AU, Robson ME, Kubo M, Ibrahim-Zada I, Batzler A, Jenkins GD, Pietrzak TL, Carlson EE, Barman P, Goetz MP, Northfelt DW, Moreno-Aspita A, Williard CV, Kalari KR, Nakamura Y, Wang L, and Weinshilboum RM (2017) SLCO1B1 polymorphisms and plasma estrone conjugates in postmenopausal women with ER+ breast cancer: genome-wide association studies of the estrone pathway. *Breast Cancer Res Treat* **164:**189-199.

Flanagan SE, Patch AM, and Ellard S (2010) Using SIFT and PolyPhen to predict loss-of-function and gain-of-function mutations. *Genet Test Mol Biomarkers* **14:**533-537.

Fowler DM and Fields S (2014) Deep mutational scanning: a new style of protein science. *Nat Methods* **11:**801-807.

Gaedigk A, Ingelman-Sundberg M, Miller NA, Leeder JS, Whirl-Carrillo M, Klein TE, and PharmVar Steering C (2018) The Pharmacogene Variation (PharmVar) Consortium:

Incorporation of the Human Cytochrome P450 (CYP) Allele Nomenclature Database. *Clin Pharmacol Ther* **103:**399-401.

Giacomini KM, Balimane PV, Cho SK, Eadon M, Edeki T, Hillgren KM, Huang SM, Sugiyama Y, Weitz D, Wen Y, Xia CQ, Yee SW, Zimdahl H, Niemi M, and International Transporter C (2013) International Transporter Consortium commentary on clinically important transporter polymorphisms. *Clin Pharmacol Ther* **94:**23-26.

Hong M, Li S, Zhou F, Thomas PE, and You G (2010) Putative transmembrane domain 12 of the human organic anion transporter hOAT1 determines transporter stability and maturation efficiency. *J Pharmacol Exp Ther* **332:**650-658.

Kameyama Y, Yamashita K, Kobayashi K, Hosokawa M, and Chiba K (2005) Functional characterization of SLCO1B1 (OATP-C) variants, SLCO1B1*5, SLCO1B1*15 and SLCO1B1*15+C1007G, by using transient expression systems of HeLa and HEK293 cells. *Pharmacogenet Genomics* **15:**513-522.

Kircher M, Witten DM, Jain P, O'Roak BJ, Cooper GM, and Shendure J (2014) A general framework for estimating the relative pathogenicity of human genetic variants. *Nat Genet* **46:**310-315.

Kitamura S, Maeda K, Wang Y, and Sugiyama Y (2008) Involvement of multiple transporters in the hepatobiliary transport of rosuvastatin. *Drug Metab Dispos* **36:**2014-2023.

Lek M, Karczewski KJ, Minikel EV, Samocha KE, Banks E, Fennell T, O'Donnell-Luria AH, Ware JS, Hill AJ, Cummings BB, Tukiainen T, Birnbaum DP, Kosmicki JA, Duncan LE, Estrada K, Zhao F, Zou J, Pierce-Hoffman E, Berghout J, Cooper DN, Deflaux N, DePristo M, Do R, Flannick J, Fromer M, Gauthier L, Goldstein J, Gupta N, Howrigan D, Kiezun A, Kurki MI, Moonshine AL, Natarajan P, Orozco L, Peloso GM, Poplin R, Rivas MA, Ruano-Rubio V, Rose SA, Ruderfer DM, Shakir K, Stenson PD, Stevens C, Thomas BP, Tiao G, Tusie-Luna MT, Weisburd B, Won HH, Yu D, Altshuler DM, Ardissino D, Boehnke M, Danesh J, Donnelly S, Elosua R, Florez JC, Gabriel SB, Getz G, Glatt SJ, Hultman CM, Kathiresan S, Laakso M, McCarroll S, McCarthy MI, McGovern D, McPherson R, Neale BM, Palotie A, Purcell SM, Saleheen D, Scharf JM, Sklar P, Sullivan PF, Tuomilehto J, Tsuang MT, Watkins HC, Wilson JG, Daly MJ, MacArthur DG, and Exome Aggregation C (2016) Analysis of protein-coding genetic variation in 60,706 humans. *Nature* **536:**285-291.

Li F, Wang L, Burgess RJ, and Weinshilboum RM (2008) Thiopurine S-methyltransferase pharmacogenetics: autophagy as a mechanism for variant allozyme degradation. *Pharmacogenet Genomics* **18:**1083-1094.

Matreyek KA, Starita LM, Stephany JJ, Martin B, Chiasson MA, Gray VE, Kircher M, Khechaduri A, Dines JN, Hause RJ, Bhatia S, Evans WE, Relling MV, Yang W, Shendure J, and Fowler DM (2018) Multiplex assessment of protein variant abundance by massively parallel sequencing. *Nat Genet* **50:**874-882.

Matreyek KA, Stephany JJ, and Fowler DM (2017) A platform for functional assessment of large variant libraries in mammalian cells. *Nucleic Acids Res* **45:**e102.

Moyer AM, de Andrade M, Faubion SS, Kapoor E, Dudenkov T, Weinshilboum RM, and Miller VM (2018) SLCO1B1 genetic variation and hormone therapy in menopausal women. *Menopause* **25:**877-882.

Niemi M (2010) Transporter pharmacogenetics and statin toxicity. *Clin Pharmacol Ther* **87:**130-133.

Oshiro C, Mangravite L, Klein T, and Altman R (2010) PharmGKB very important pharmacogene: SLCO1B1. *Pharmacogenet Genomics* **20:**211-216.

Parvez MM, Jung JA, Shin HJ, Kim DH, and Shin JG (2016) Characterization of 22 Antituberculosis Drugs for Inhibitory Interaction Potential on Organic Anionic Transporter Polypeptide (OATP)-Mediated Uptake. *Antimicrob Agents Chemother* **60:**3096-3105.

Suiter CC, Moriyama T, Matreyek KA, Yang W, Scaletti ER, Nishii R, Yang W, Hoshitsuki K, Singh M, Trehan A, Parish C, Smith C, Li L, Bhojwani D, Yuen LYP, Li CK, Li CH, Yang YL, Walker GJ, Goodhand JR, Kennedy NA, Klussmann FA, Bhatia S, Relling MV, Kato M, Hori H, Bhatia P, Ahmad T, Yeoh AEJ, Stenmark P, Fowler DM, and Yang JJ (2020) Massively parallel variant characterization identifies NUDT15 alleles associated with thiopurine toxicity. *Proc Natl Acad Sci U S A* **117:**5394-5401.

Tirona RG, Leake BF, Merino G, and Kim RB (2001) Polymorphisms in OATP-C: identification of multiple allelic variants associated with altered transport activity among European- and African-Americans. *J Biol Chem* **276:**35669-35675.

van de Steeg E, Greupink R, Schreurs M, Nooijen IH, Verhoeckx KC, Hanemaaijer R, Ripken D, Monshouwer M, Vlaming ML, DeGroot J, Verwei M, Russel FG, Huisman MT, and Wortelboer HM (2013) Drug-drug interactions between rosuvastatin and oral antidiabetic drugs occurring at the level of OATP1B1. *Drug Metab Dispos* **41:**592-601.

Vaser R, Adusumalli S, Leng SN, Sikic M, and Ng PC (2016) SIFT missense predictions for genomes. *Nat Protoc* **11:**1-9.

Voora D, Shah SH, Spasojevic I, Ali S, Reed CR, Salisbury BA, and Ginsburg GS (2009) The SLCO1B1*5 genetic variant is associated with statin-induced side effects. *J Am Coll Cardiol* **54:**1609-1616.

Wang L, Nguyen TV, McLaughlin RW, Sikkink LA, Ramirez-Alvarado M, and Weinshilboum RM (2005) Human thiopurine S-methyltransferase pharmacogenetics: variant allozyme misfolding and aggresome formation. *Proc Natl Acad Sci U S A* **102:**9394-9399.

Wang L, Yee VC, and Weinshilboum RM (2004) Aggresome formation and pharmacogenetics: sulfotransferase 1A3 as a model system. *Biochem Biophys Res Commun* **325:**426-433.

Wrenbeck EE, Klesmith JR, Stapleton JA, Adeniran A, Tyo KE, and Whitehead TA (2016) Plasmid-based one-pot saturation mutagenesis. *Nat Methods* **13:**928-930.

Zhang L, Sarangi V, Moon I, Yu J, Liu D, Devarajan S, Reid JM, Kalari KR, Wang L, and Weinshilboum R (2020) CYP2C9 and CYP2C19: Deep Mutational Scanning and Functional Characterization of Genomic Missense Variants. *Clin Transl Sci* **13:**727-742.

DMD Fast Forward. Published on March 3, 2021 as DOI: 10.1124/dmd.120.000264
This article has not been copyedited and formatted. The final version may differ from this version.

Footnote

This study was funded by National Institute of General Medical Sciences (NIGMS) [Grant GM61388] (The Pharmacogenomics Research Network); National Institute of General Medical Sciences (NIGMS) [Grant GM28157]; National Institute on Alcohol Abuse and Alcoholism (NIAAA) [Grants AA27486, AA2850]; National Institute of General Medical Sciences (NIGMS) R01 [Grant GM125633]; and by the Mayo Clinic Center for Individualized Medicine.

CONFLICT OF INTEREST: Both Drs. Weinshilboum and Wang are co-founders of and stockholders in OneOme, LLC. Other authors have no conflicts of interest to declare.

DMD Fast Forward. Published on March 3, 2021 as DOI: 10.1124/dmd.120.000264
This article has not been copyedited and formatted. The final version may differ from this version.

Figure legends

Figure 1. Flow cytometry of *SLCO1B1* constructs with known variants and FACS-sorting of pooled *SLCO1B1* variant libraries.

(**A**) The *SLCO1B1* expression cassette is depicted diagrammatically. When this vector is integrated into a "landing pad" in HEK293 cells, it results in the expression of recombinant protein that is labeled with green fluorescent protein (GFP) labeled *SLCO1B1*, while the cell itself will express mCherry, so the ratio of GFP to mCherry serves as an indication of the stability of the expressed protein, i.e. the higher that ratio, the more stable the protein encoded by the expressed variants. (**B&C)** Flow cytometry analysis of blue fluorescent protein BFP^- /$mCherrry^+$ cells that had integrated wild-type or known damaging variant such as *SLCO1B1*2***.** Note that for the wild-type (WT) protein, most of the cells eluted toward higher GFP/mCherry ratios, while cells containing damaging variants eluted at significantly lower GFP/mCherry ratios than did cells expressing the WT. Mean GFP/mCherry ratios for those variants were consistent with Western Blot results obtained during our previous study. (**D)** Cells integrating *SLCO1B1* pooled variant libraries were sorted into 4 bins based on their GFP/mCherry ratios. The variants were categorized into three groups: severely damaging variants fell into bin 1, damaging variant fell into bin 2 and bin 3, and tolerated variants fell into bin 4. Gates were set based on WT *SLCO1B1* and *SLCO1B1*2*. Pools of sorted cells in each bin were collect and were used as input material for subsequent amplicon DNA sequencing.

Figure 2. Protein abundance scores for 137 *SLCO1B1* variants.

DMD Fast Forward. Published on March 3, 2021 as DOI: 10.1124/dmd.120.000264
This article has not been copyedited and formatted. The final version may differ from this version.

Abundance score values for *SLCO1B1* variants. Variants having abundance scores less than or equal to 0.5728 *SLCO1B1* (1296C>A) were classified as "severely damaging" variants, while variants having abundance scores equal to or above 0.5768 (*SLCO1B1*1B*, 388A>G, rs2306283) but less than 0.6015 (*SLCO1B1*27*, 1200C>G, rs59113707) were classified as "damaging". Variants having abundance scores higher than 0.6015 were classified as "tolerated". The results shown are averages abundance scores for four replicates. SD values are listed in **Supplemental Table S1**.

Figure 3. Variant frequencies by bin for "severely" damaging *SLCO1B1* variants.

The Figure shows variant frequencies by bin for the six newly identified "severely" damaging variants (1462G>A, 1246G>A, 215G>A, 1508A>G 1828C>T, and 1296C>A) for *SLCO1B1* as well as their distribution into each of the four bins, as well as similar data for the common *SLCO1B1*5* allele.

Figure 4. Validation of *SLCO1B1* variants identified as containing severely damaging variants.

(A) Western blot validation of *SLCO1B1* variants identified as containing severely damaging variants. The protein expression of *SLCO1B1* in $BFP^-/mCherry^+$ cells integrating severely damaging variants were validated by Western blot analysis. mCherry was used as a loading control. A control lane contained wild-type (WT) *SLCO1B1*. (**B**) Concentration-dependent uptake of estradiol 17-β-D-glucuronide by *SLCO1B1* WT $BFP^-/mCherry^+$ cells and the six newly

DMD Fast Forward. Published on March 3, 2021 as DOI: 10.1124/dmd.120.000264
This article has not been copyedited and formatted. The final version may differ from this version.

identified severely damaging *SLCO1B1* variant $BFP^-/mCherry^+$ cells after 1 minute incubations. The quantity of radioactively labeled estradiol 17-β-D-glucuronide that accumulated within the cells was determined by liquid scintillation counting. The data are expressed in counts per minute (CPM) normalized by the amount of protein content in milligrams. Data are presented as mean uptake for three replicate experiments. (**C**) The bar graph shows the uptake of estradiol 17-β-D-glucuronide (24 nM) for variants in *SLCO1B1* TM4 in $BFP^-/mCherry^+$ cells after 1 minute incubations. The uptake activities of variants in severely damaging variants against WT were tested by one-way ANOVA, **** $p<0.0001$. (**D**) Concentration-dependent uptake of estradiol 17-β-D-glucuronide for variants in *SLCO1B1* transmembrane domain 4 (TM4) in $BFP^-/mCherry^+$ cells after 1 minute incubations. Data are presented as mean ± S.D. of counts per minute (CPM) / mg protein for three replicated experiments. (**E**) The bar graph shows the uptake of estradiol 17-β-D-glucuronide (24 nM) for variants in *SLCO1B1* TM4 in $BFP^-/mCherry^+$ cells after 1 minute incubations. The uptake activities of variants in TM4 against WT were tested by one-way ANOVA, * $p<0.05$, **** $p<0.0001$.

Figure 1

DMD Fast Forward. Published on March 3, 2021 as DOI: 10.1124/dmd.120.000264
This article has not been copyedited and formatted. The final version may differ from this version.

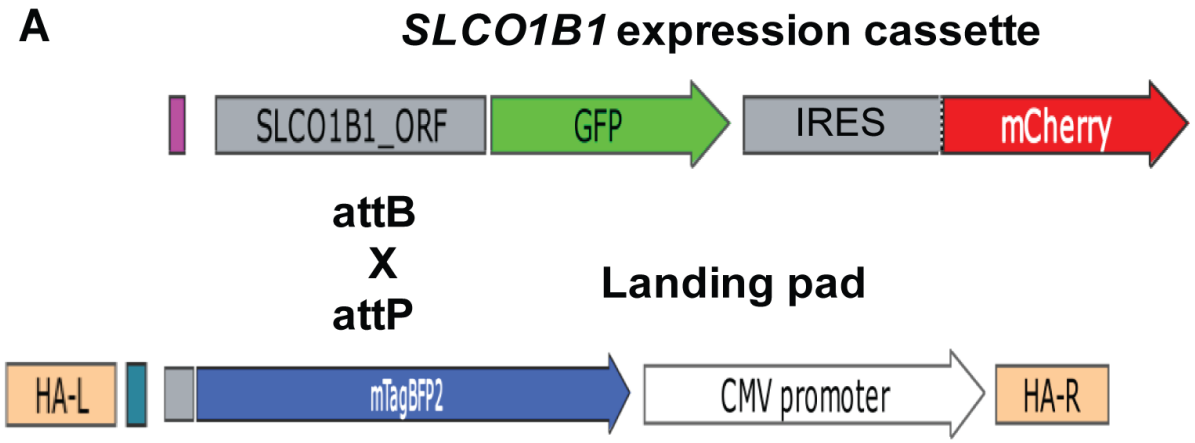

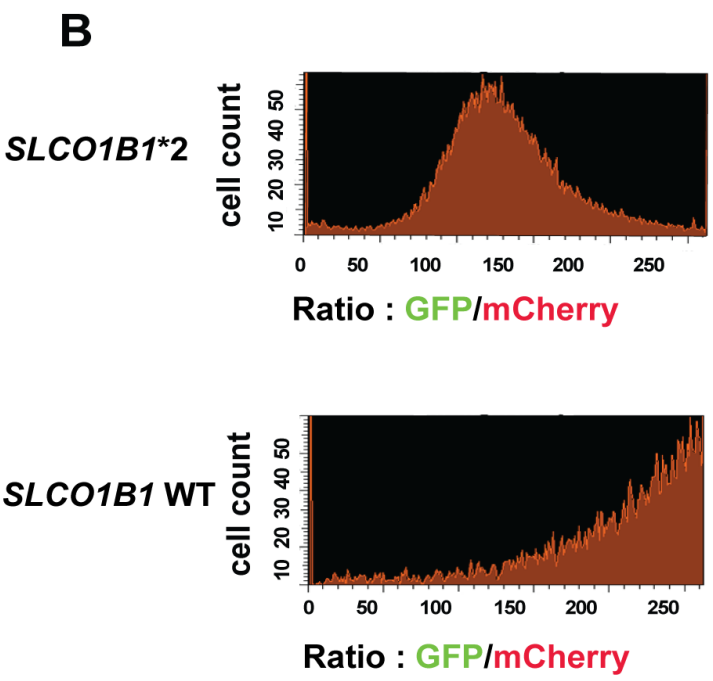

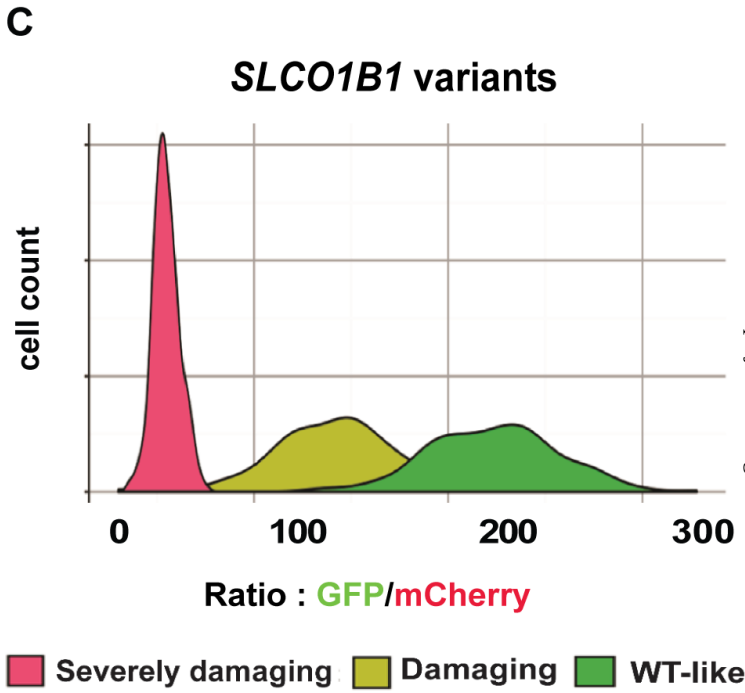

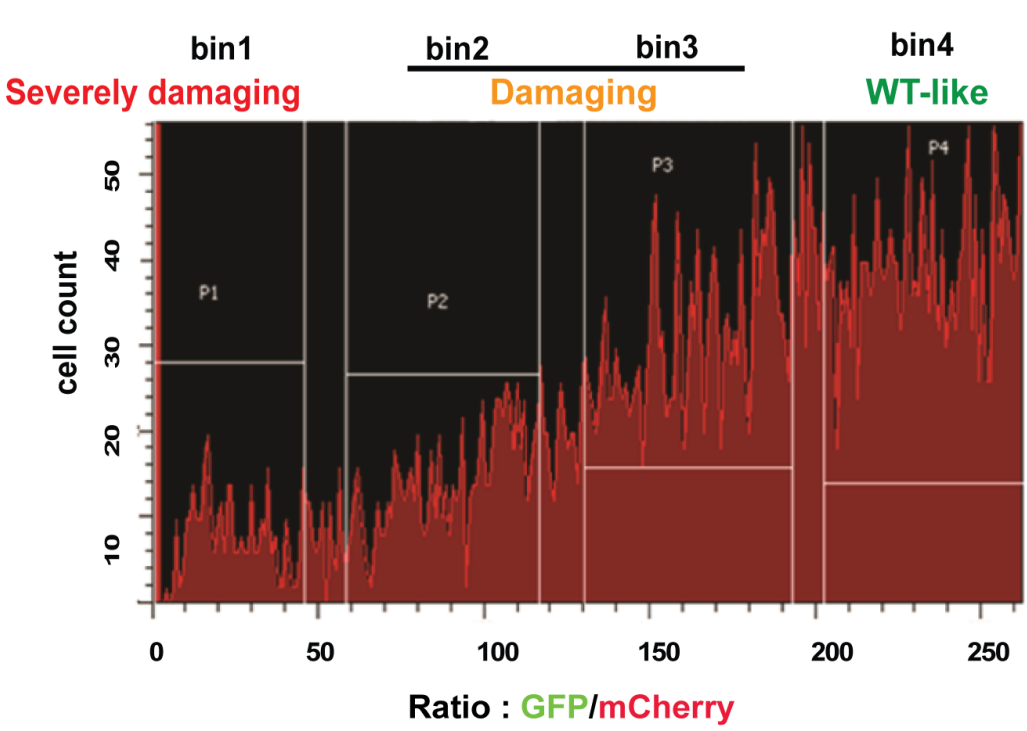

DMD Fast Forward. Published on March 3, 2021 as DOI: 10.1124/dmd.120.000264
This article has not been copyedited and formatted. The final version may differ from this version.

Figure 2

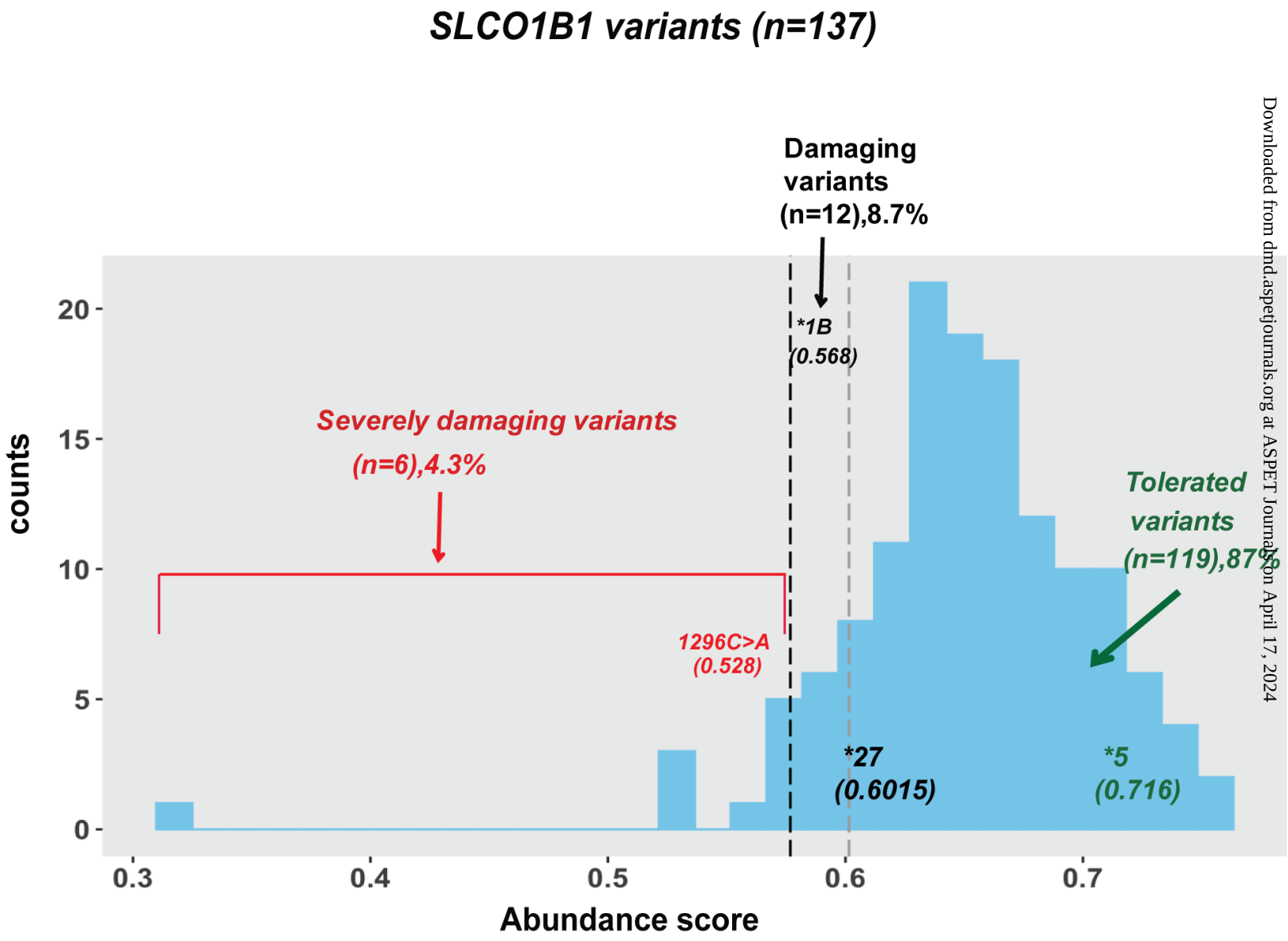

DMD Fast Forward. Published on March 3, 2021 as DOI: 10.1124/dmd.120.000264
This article has not been copyedited and formatted. The final version may differ from this version.

Figure 3

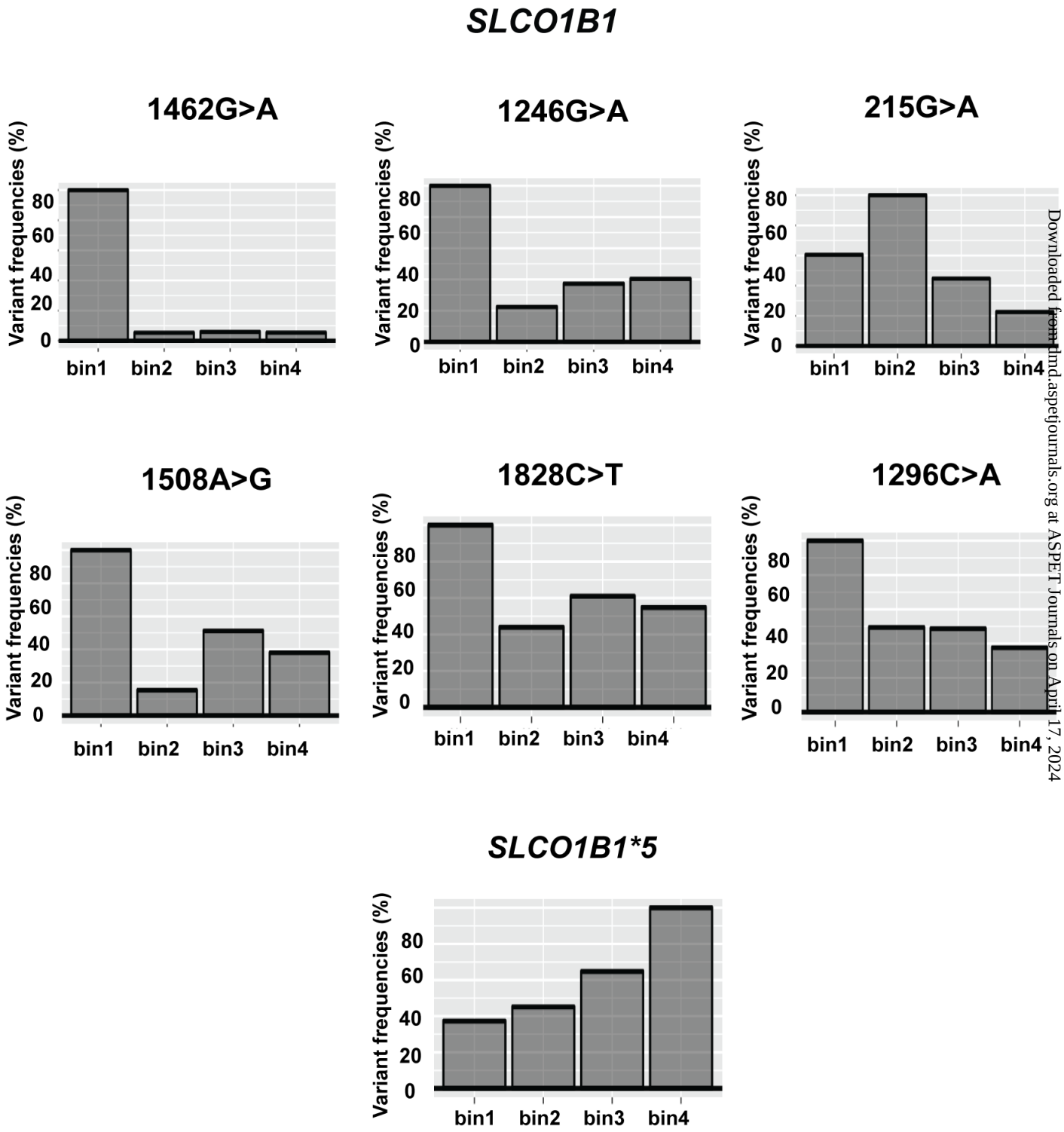

DMD Fast Forward. Published on March 3, 2021 as DOI: 10.1124/dmd.120.000264
This article has not been copyedited and formatted. The final version may differ from this version.

Figure 4

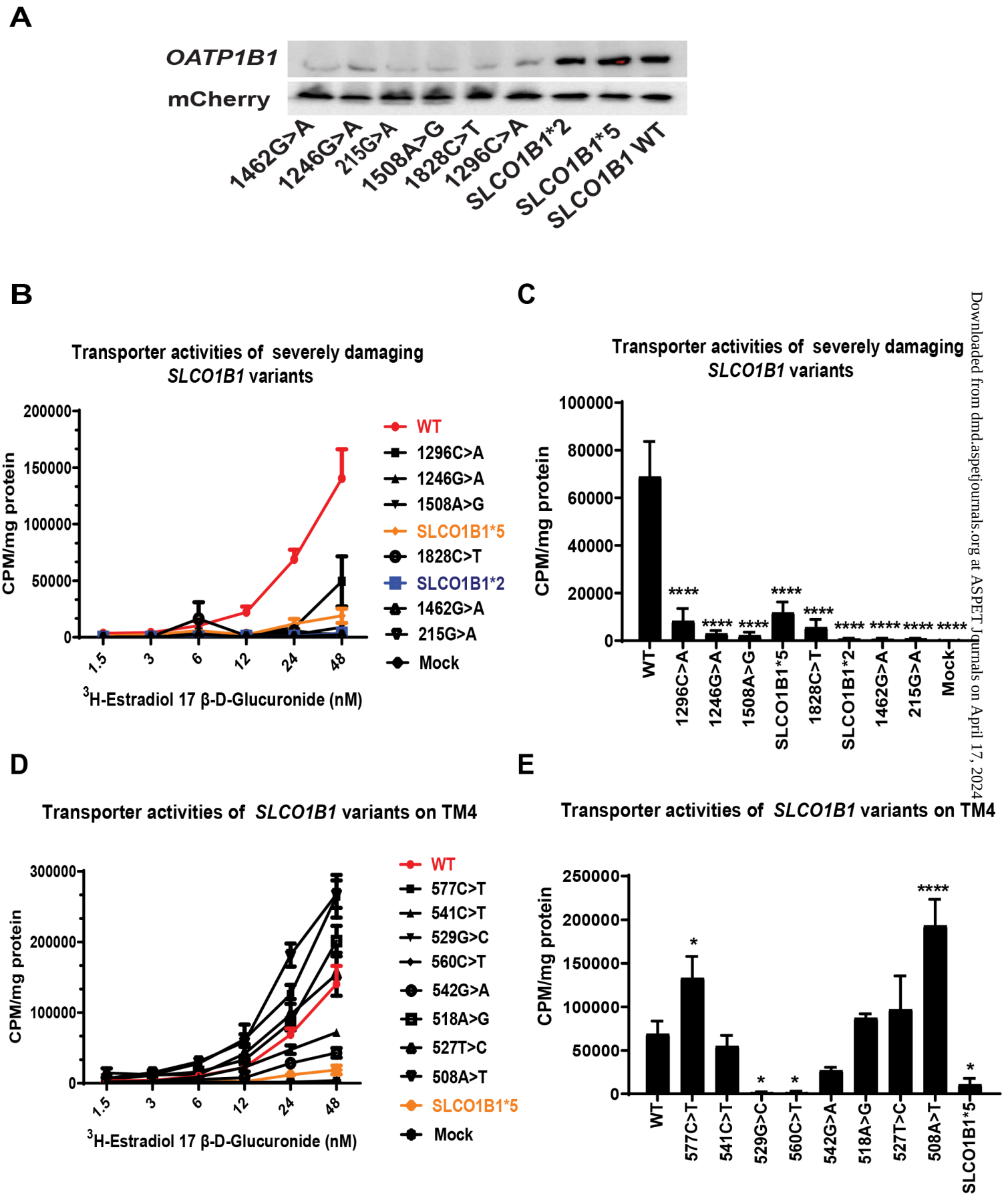

DMD Fast Forward. Published on March 3, 2021 as DOI: 10.1124/dmd.120.000264
This article has not been copyedited and formatted. The final version may differ from this version.

Figure 5. Protein abundance scores of *SLCO1B1* variants from ExAC Browser and Mayo Right 10K Study

EXACT cDNA	EXACT Amino acid	RSID	Common allele name	Allele Frequency	Right 10K (Variant Prevalence)			DMS	
					WT	Heterozygous	Homozygous	Functional Study	Abundance Score
c.1296C>A	p.Asn432Lys	rs534931824		0.000108				Severely Damaging	0.5728
c.1828C>T	p.Arg610Cys	rs748860610		5.77E-05	10082	2	0	Severely Damaging	0.5679
c.1246G>A	p.Val416Met	rs77468276		1.66E-05				Severely Damaging	0.5225
c.1462G>A	p.Gly488Ser	rs774471564		1.65E-05				Severely Damaging	0.3205
c.1508A>G	p.Asn503Ser	rs368423244		1.65E-05				Severely Damaging	0.5332
c.215G>A	p.Ser72Asn	rs780686282		8.77E-06				Severely Damaging	0.5322
c.388A>G	p.Asn130Asp	rs2306283	*SLCO1B1*1B*	0.4795	3525	4920	1639	Damaging	0.5768
c.1200C>G	p.Phe400Leu	rs59113707	*SLCO1B1*27*	0.004341				Damaging	0.6015
c.169C>T	p.Arg57Trp	rs139257324	*SLCO1B1*33*	0.000108				Damaging	0.5848
c.671T>A	p.Phe224Tyr	rs756431817		7.42E-05				Damaging	0.5925
c.1015G>C	p.Val339Leu	rs758315826	*SLCO1B1*61*	3.42E-05				Damaging	0.577
c.235C>T	p.Leu79Phe	rs370130036		3.40E-05				Damaging	0.5867
c.695A>C	p.Lys232Thr	rs374328647		3.30E-05				Damaging	0.594
c.38C>A	p.Ala13Glu	rs778214174		2.49E-05				Damaging	0.5994
c.593A>G	p.Asp198Gly	rs376755211		2.47E-05				Damaging	0.5944
c.991A>G	p.Ser331Gly	rs774845200		1.79E-05				Damaging	0.5875
c.1796G>A	p.Cys599Tyr	rs531488136		1.65E-05				Damaging	0.5799
c.154A>G	p.Ile52Val	rs762874802		1.65E-05				Damaging	0.5984
c.521T>C	p.Val174Ala	rs4149056	*SLCO1B1*5*	0.1294	7057	2768	259	TOLERATED	0.7167
c.463C>A	p.Pro155Thr	rs11045819	*SLCO1B1*4*	0.1166	7181	2656	247	TOLERATED	0.6718
c.1929A>C	p.Leu643Phe	rs34671512	*SLCO1B1*19*	0.04632	9074	986	24	TOLERATED	0.7172
c.733A>G	p.Ile245Val	rs11045852	*SLCO1B1*24*	0.007622				TOLERATED	0.6492
c.633A>G	p.Ile211Met	rs201722521		0.004007	10074	9	1	TOLERATED	0.7314
c.1463G>C	p.Gly488Ala	rs59502379	*SLCO1B1*9*	0.003196				TOLERATED	0.6747
c.1495A>G	p.Ile499Val	rs74064213		0.002482				TOLERATED	0.6654
c.664A>G	p.Ile222Val	rs79135870	*SLCO1B1*29*	0.00099				TOLERATED	0.7112
c.317T>C	p.Ile106Thr	rs200227560		0.000693	10076	8	0	TOLERATED	0.6273
c.758G>A	p.Arg253Gln	rs11045853	*SLCO1B1*25*	0.00042	10083	1	0	TOLERATED	0.6323

DMD Fast Forward. Published on March 3, 2021 as DOI: 10.1124/dmd.120.000264
This article has not been copyedited and formatted. The final version may differ from this version.

c.170G>A	p.Arg57Gln	rs61760182		0.000356	10083	1	0	TOLERATED	0.7455
c.452A>G	p.Asn151Ser	rs2306282	*SLCO1B1 *16*	0.000347				TOLERATED	0.6227
c.1034C>T	p.Thr345Met	rs61760243		0.000253	10082	2	0	TOLERATED	0.6214
c.2032C>T	p.His678Tyr	rs200995543	*SLCO1B1*34*	0.000249				TOLERATED	0.6821
c.1309G>A	p.Gly437Arg	rs142965323	*SLCO1B1*26*	0.0002	10078	6	0	TOLERATED	0.6296
c.1622A>T	p.Gln541Leu	rs71581988		0.000132				TOLERATED	0.6445
c.2045C>T	p.Ser682Phe	rs140790673	*SLCO1B1*28*	0.000108				TOLERATED	0.6382
c.1007C>G	p.Pro336Arg	rs72559747		0.000104	10083	1	0	TOLERATED	0.634
c.1732G>A	p.Val578Ile	rs201001269		9.10E-05	10083	1	0	TOLERATED	0.6291
c.1322C>A	p.Thr441Asn	rs141779296		8.38E-05				TOLERATED	0.6661
c.1226A>G	p.Lys409Arg	rs199859384		8.32E-05				TOLERATED	0.7054
c.1373A>T	p.Tyr458Phe	rs750798503		7.44E-05				TOLERATED	0.687
c.601A>G	p.Lys201Glu	rs556914358		7.42E-05				TOLERATED	0.6046
c.518A>G	p.Tyr173Cys	rs141467543		7.42E-05				TOLERATED	0.6644
c.1213G>A	p.Val405Ile	rs376060151		6.67E-05				TOLERATED	0.6274
c.1865C>T	p.Ser622Leu	rs368052440		6.65E-05				TOLERATED	0.6501
c.638A>G	p.Asn213Ser	rs372477451		6.61E-05	10083	1	0	TOLERATED	0.6644
c.455G>C	p.Arg152Thr	rs145144129		5.79E-05				TOLERATED	0.7588
c.639T>A	p.Asn213Lys	rs752897663		5.78E-05				TOLERATED	0.6908
c.542G>A	p.Arg181His	rs142101690		5.77E-05				TOLERATED	0.7027
c.211G>A	p.Gly71Arg	rs373327528		5.18E-05	10081	3	0	TOLERATED	0.7462
c.1080C>G	p.Phe360Leu	rs140674443		4.99E-05				TOLERATED	0.6719
c.66A>T	p.Arg22Ser	rs142087529		4.99E-05				TOLERATED	0.71
c.410C>T	p.Ser137Leu	rs151204465		4.96E-05	10083	1	0	TOLERATED	0.659
c.152C>T	p.Ser51Phe	rs769900186		4.96E-05				TOLERATED	0.7129
c.577C>T	p.Leu193Phe	rs376996580		4.95E-05				TOLERATED	0.6597
c.1978G>C	p.Glu660Gln	rs368443740		4.20E-05				TOLERATED	0.6279
c.1178G>A	p.Gly393Glu	rs768154342		4.19E-05				TOLERATED	0.6814
c.380C>G	p.Thr127Ser	rs569028384	*SLCO1B1*33*	4.14E-05	10083	1	0	TOLERATED	0.7218
c.298G>A	p.Gly100Ser	rs144508550		4.13E-05				TOLERATED	0.6233
c.850A>G	p.Asn284Asp	rs779059572		4.12E-05				TOLERATED	0.651
c.508A>T	p.Met170Leu	rs764816711		4.12E-05				TOLERATED	0.6552
c.238G>T	p.Val80Leu	rs781021072		3.39E-05				TOLERATED	0.6433
c.1739G>A	p.Arg580Gln	rs763991908		3.31E-05				TOLERATED	0.6099

DMD Fast Forward. Published on March 3, 2021 as DOI: 10.1124/dmd.120.000264
This article has not been copyedited and formatted. The final version may differ from this version.

c.385A>G	p.Ile129Val	rs759691773		3.31E-05				TOLERATED	0.6807
c.1573C>T	p.Pro525Ser	rs71581987		3.30E-05				TOLERATED	0.6178
c.766G>A	p.Gly256Arg	rs754247932		3.30E-05				TOLERATED	0.6289
c.728G>A	p.Ser243Asn	rs558073276		3.30E-05				TOLERATED	0.6366
c.485G>A	p.Cys162Tyr	rs138374684		0.000033	10083	1	0	TOLERATED	0.6533
c.1829G>A	p.Arg610His	rs769518588		0.000033				TOLERATED	0.6645
c.743C>T	p.Thr248Ile	rs774398133		3.30E-05				TOLERATED	0.6676
c.703G>A	p.Val235Met	rs147421160		0.000033	10082	2	0	TOLERATED	0.6918
c.106C>T	p.Leu36Phe	rs751767004		3.30E-05				TOLERATED	0.7133
c.992G>A	p.Ser331Asn	rs760313969		2.68E-05	10082	2	0	TOLERATED	0.6478
c.212G>A	p.Gly71Glu	rs540723056		2.61E-05				TOLERATED	0.7123
c.250G>T	p.Val84Leu	rs750031541		2.52E-05				TOLERATED	0.6253
c.1878G>C	p.Leu626Phe	rs200526972		2.51E-05	10083	1	0	TOLERATED	0.6499
c.1087G>A	p.Val363Ile	rs764782382		2.49E-05	10083	1	0	TOLERATED	0.6104
c.1742C>T	p.Ala581Val	rs751309254		2.49E-05				TOLERATED	0.6202
c.944G>A	p.Gly315Glu	rs373619379		2.49E-05				TOLERATED	0.6837
c.904A>T	p.Asn302Tyr	rs770854976		2.48E-05				TOLERATED	0.6022
c.314G>T	p.Gly105Val	rs773434165		2.48E-05				TOLERATED	0.6312
c.629G>T	p.Gly210Val	rs766417954		2.48E-05				TOLERATED	0.6446
c.1671G>A	p.Met557Ile	rs770420484		2.48E-05				TOLERATED	0.6606
c.1441T>C	p.Tyr481His	rs745708956		2.48E-05	10083	1	0	TOLERATED	0.6722
c.1444A>G	p.Ile482Val	rs769428117		2.48E-05				TOLERATED	0.7065
c.1729A>G	p.Met577Val	rs371102023		2.48E-05				TOLERATED	0.7287
c.778C>T	p.Leu260Phe	rs756955511		2.47E-05				TOLERATED	0.6275
c.1793C>T	p.Thr598Met	rs201861991		2.47E-05	10082	2	0	TOLERATED	0.6285
c.598G>A	p.Ala200Thr	rs540112224		2.47E-05				TOLERATED	0.6502
c.541C>T	p.Arg181Cys	rs138965366		2.47E-05				TOLERATED	0.6519
c.1616C>T	p.Ala539Val	rs558485740	*SLCO1B1*46*	2.47E-05				TOLERATED	0.6642
c.875C>T	p.Ala292Val	rs778642823		2.47E-05				TOLERATED	0.6772
c.1784T>C	p.Ile595Thr	rs139026094		2.47E-05				TOLERATED	0.7203
c.1564G>T	p.Gly522Cys	rs112909948		2.47E-05				TOLERATED	0.7355
c.981G>T	p.Gln327His			1.90E-05				TOLERATED	0.6342
c.986T>G	p.Phe329Cys	rs764497327		1.84E-05				TOLERATED	0.6703
c.1966A>G	p.Ile656Val	rs757219127		1.69E-05				TOLERATED	0.635

DMD Fast Forward. Published on March 3, 2021 as DOI: 10.1124/dmd.120.000264
This article has not been copyedited and formatted. The final version may differ from this version.

c.1159G>A	p.Ala387Thr	rs775082787		1.69E-05				TOLERATED	0.6456
c.1319T>G	p.Met440Arg	rs139797371	*SLCO1B1*43*	1.68E-05	10082	2	0	TOLERATED	0.682
c.1298A>G	p.Lys433Arg	rs772057264		1.67E-05				TOLERATED	0.639
c.193C>G	p.Leu65Val	rs766895771		1.67E-05	10082	2	0	TOLERATED	0.6759
c.1214T>C	p.Val405Ala			1.67E-05				TOLERATED	0.6979
c.1100A>G	p.Tyr367Cys	rs757036708		1.66E-05				TOLERATED	0.6216
c.481G>A	p.Gly161Ser	rs749356996		1.66E-05				TOLERATED	0.6364
c.1076T>C	p.Val359Ala	rs147750118		1.66E-05				TOLERATED	0.6436
c.47C>T	p.Ser16Leu	rs753618172		1.66E-05				TOLERATED	0.7199
c.128T>C	p.Leu43Pro	rs770472561		1.65E-05				TOLERATED	0.6088
c.1729A>C	p.Met577Leu	rs371102023		1.65E-05				TOLERATED	0.6142
c.1628T>G	p.Leu543Trp	rs72661137		1.65E-05				TOLERATED	0.6165
c.1765A>G	p.Ile589Val	rs779674373		1.65E-05				TOLERATED	0.6209
c.529G>C	p.Gly177Arg	rs750234871		1.65E-05				TOLERATED	0.6362
c.395C>T	p.Ser132Leu	rs763429608		1.65E-05				TOLERATED	0.6368
c.560C>T	p.Pro187Leu	rs779195754		1.65E-05				TOLERATED	0.641
c.1384G>A	p.Asp462Asn	rs778655808		1.65E-05				TOLERATED	0.6418
c.674C>T	p.Thr225Ile	rs370943869		1.65E-05				TOLERATED	0.6468
c.1784T>G	p.Ile595Ser	rs139026094		1.65E-05				TOLERATED	0.6508
c.808A>C	p.Ile270Leu	rs201438350		1.65E-05				TOLERATED	0.6511
c.331A>C	p.Thr111Pro	rs759510840		1.65E-05				TOLERATED	0.6515
c.1837T>C	p.Cys613Arg	rs377350683	*SLCO1B1*30*	1.65E-05				TOLERATED	0.6571
c.1778C>G	p.Ala593Gly	rs768644633		1.65E-05				TOLERATED	0.6588
c.763G>C	p.Val255Leu	rs766769140		1.65E-05	10083	1	0	TOLERATED	0.6662
c.145A>G	p.Lys49Glu	rs745339838		1.65E-05				TOLERATED	0.6715
c.1856C>T	p.Thr619Ile	rs760486881		1.65E-05				TOLERATED	0.6726
c.1430A>G	p.Asn477Ser	rs781211732		1.65E-05				TOLERATED	0.6797
c.1664A>G	p.His555Arg	rs781111529		1.65E-05				TOLERATED	0.6803
c.133G>A	p.Ala45Thr	rs555367334		1.65E-05	10083	1	0	TOLERATED	0.681
c.1781T>C	p.Leu594Pro	rs761720319		1.65E-05				TOLERATED	0.6918
c.527T>C	p.Met176Thr	rs548326440		1.65E-05				TOLERATED	0.6921
c.1805G>T	p.Trp602Leu	rs778178385		1.65E-05	10082	2	0	TOLERATED	0.6926
c.1589G>A	p.Cys530Tyr	rs184762532		1.65E-05				TOLERATED	0.6941
c.1451C>A	p.Pro484His	rs568944276		1.65E-05				TOLERATED	0.6949

DMD Fast Forward. Published on March 3, 2021 as DOI: 10.1124/dmd.120.000264
This article has not been copyedited and formatted. The final version may differ from this version.

c.610C>T	p.His204Tyr	rs767379248	1.65E-05				TOLERATED	0.6953
c.713G>A	p.Gly238Glu	rs374113543	1.65E-05	10081	3	0	TOLERATED	0.7046
c.1414C>T	p.Pro472Ser	rs746507861	1.65E-05				TOLERATED	0.7267
c.1612G>A	p.Val538Ile	rs760163504	1.65E-05				TOLERATED	0.7384
c.1465T>A	p.Cys489Ser	rs144733213	1.65E-05				TOLERATED	0.7535
c.222A>T	p.Glu74Asp	rs745392993	9.18E-06				TOLERATED	0.6631
c.1000A>T	p.Thr334Ser	rs77871475	8.75E-06				TOLERATED	0.6152